

Quasi one dimensional transport in individual electrospun composite nanofibers

A. Avnon, B. Wang, S. Zhou, V. Datsyuk, S. Trotsenko, N. Grabbert, and H.-D. Ngo

Citation: *AIP Advances* **4**, 017110 (2014); doi: 10.1063/1.4862168

View online: <https://doi.org/10.1063/1.4862168>

View Table of Contents: <http://aip.scitation.org/toc/adv/4/1>

Published by the [American Institute of Physics](#)

Articles you may be interested in

[Physical origin of nonlinear transport in organic semiconductor at high carrier densities](#)

Journal of Applied Physics **116**, 164504 (2014); 10.1063/1.4897916

[Nonlinear transport in quasi-one-dimensional Nb₂PdS₅ nanowires](#)

Applied Physics Letters **105**, 172603 (2014); 10.1063/1.4901005

HAVE YOU HEARD?

Employers hiring scientists and
engineers trust

PHYSICS TODAY | JOBS

www.physicstoday.org/jobs



Quasi one dimensional transport in individual electrospun composite nanofibers

A. Avnon,^{1,a} B. Wang,² S. Zhou,² V. Datsyuk,¹ S. Trotsenko,¹ N. Grabbert,³ and H.-D. Ngo³

¹*Institut für Experimentalphysik, Freie Universität Berlin, Arnimallee 14, 14195 Berlin, Germany*

²*Research Center of Microperipheric Technologies, Technische Universität Berlin, TiB4/2-1, Gustav-Meyer-Allee 25, 13355 Berlin, Germany*

³*Microsystem Engineering (FB I), University of Applied Sciences, Wilhelminenhofstr. 74 (C 525), 12459 Berlin, Germany*

(Received 17 November 2013; accepted 30 December 2013; published online 9 January 2014)

We present results of transport measurements of individual suspended electrospun nanofibers Poly(methyl methacrylate)-multiwalled carbon nanotubes. The nanofiber is comprised of highly aligned consecutive multiwalled carbon nanotubes. We have confirmed that at the range temperature from room temperature down to ~ 60 K, the conductance behaves as power-law of temperature with an exponent of $\alpha \sim 2.9-10.2$. The current also behaves as power law of voltage with an exponent of $\beta \sim 2.3-8.6$. The power-law behavior is a footprint for one dimensional transport. The possible models of this confined system are discussed. Using the model of Luttinger liquid states in series, we calculated the exponent for tunneling into the bulk of a single multiwalled carbon nanotube $\alpha_{bulk} \sim 0.06$ which agrees with theoretical predictions. © 2014 Author(s). All article content, except where otherwise noted, is licensed under a Creative Commons Attribution 3.0 Unported License. [<http://dx.doi.org/10.1063/1.4862168>]

As nanosized devices are becoming more and more significant, electron-electron interactions due to the size confinement, become more important for transport and worthy of consideration and discussion. Electron-electron interactions are a main player in one dimensional transport bringing about behavior different from the classic Fermi liquid. Different kinds of behaviors are associated with electron-electron interactions: Luttinger liquid behavior resulting from repulsive short range electron-electron interactions,¹⁻⁵ Wigner crystal behavior resulting from long range Coulomb interaction⁶ or environmental Coulomb blockade.⁷ The characteristic fingerprint for quasi- one dimensional behavior is a power-law dependence of the conductance with temperature and of the current with applied potential. The power-law was observed in various systems ranging from carbon nanotubes,^{1-3,6-8} conducting conjugated polymer nanowires,^{5,9-11} semiconductors nanowires^{4,12,13} and fractional quantum Hall edge states.¹⁴

One way of obtaining continuous nanofibers is by electrospinning.^{15,16} During the process, the nanofibers can be filled with nanosized fillers, resulting in highly aligned one dimensional nanofibers. In that respect, it is a unique system which creates a long nanochain of confined conduction. Doping insulating polymers such as Poly(methyl methacrylate) (PMMA) with multiwalled carbon nanotubes (MWCNTs) creates a confined one dimensional system. This system can present either short range or long range electron-electron interactions depending on the temperature and morphology which can further elucidate the nature of one dimensional behavior.

In this paper, we report our transport studies of individual suspended electrospun MWCNT-PMMA nanofiber. We perform analysis of early experimental data for a MWCNT-PMMA nanofiber

^aCorresponding author; electronic address: avnon@phys.fu-berlin.de

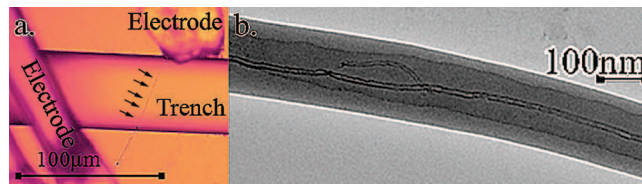


FIG. 1. (a). Optical image of a representing individual MWCNT-PMMA nanofiber. The nanofiber is visible as a faint black line over the trench and is connected by direct bonds. To assist the eye, the image was sharpened and arrows are pointing at the nanofiber. It can be seen that only a single nanofiber is nested across the trench. The trench width is $50 \mu\text{m}$. The total length of the nanofiber between the bonds is $\sim 100 \mu\text{m}$. (b). A transmission electron microscopy image of the nanofiber. The MWCNTs align inside the nanofiber in series and create a nanochain of conduction with minimal separation.

aiming to determine the adaptation of different models for one dimensional conductors and in particular the model for Luttinger liquid states in series.

We fabricated three samples. Two samples with 20 wt% of MWCNTs and one sample with 25 wt% of MWCNTs. For the first two samples, we dispersed 0.6g of MWCNTs purchased from Bayer Material Science -Baytubes C150^{15,17} in 60g of dimethyl acetamide (Carl Roth, GmbH) with 1g of hydroxypropyl cellulose (from Aldrich Mw 100.000) by ultrasonification for 30 minutes. 3g of PMMA (from Aldrich Mw 996.000) were dissolved in 30g of acetone. Dimethyl acetamide and acetone were used without any additional purification. For dispersion tip sonicator Sonopuls HD3100, Bandelin GmbH, equipped with a cup horn operating at 10 kHz and 100 W output power was used.¹⁶ Components were mixed together and were dispersed by ultrasonification for additional 30 minutes. Nanofibers were electrospun using Yflow®2.2.D-300 lab -scale electrospinning unit with single-nozzle electrospinning (Yflow Sistemas y Desarrollos S.L) with an injector-collector distance of 15 cm, an applied voltage of +9.5/−8.0 kV, and a flow rate of 2 ml/h. For the third sample we used 25 wt% of MWCNTs with flow rate of 1 ml/h, applied voltage of +8/−12 kV and injector-collector distance of 12 cm.

For electrical conductivity study, nanofibers were spun directly onto a highly doped Si/SiO_x substrate with 600nm oxide with prefabricated trenches. For the fabrication of the trenches, 100mm(100) wafers with one polished side were used. A cleaning process was performed using H₂SO₄+H₂O₂. After this, a photolithography process was performed. The resist thickness was $1.5 \mu\text{m}$. Trenches in width of $50 \mu\text{m}$ were etched using deep silicon etching followed by resist stripping and another cycle of H₂SO₄+H₂O₂ cleaning. For the insulation of the substrate, a 600 nm thick SiO₂ layer was deposited on the wafer using wet oxidation at 1000°C. Candidate nanofibers were located using an optical microscope and afterward were connected through direct aluminum bonding onto the nanofibers. Atomic force microscopy imaging was performed with Park XE-150 in tapping mode to determine the diameter of the nanofibers. The electrical measurements were performed with a Keithley 4200-SCS and an Oxford closed cycle cryostat with 2-probe in Helium ambiance.

Fig. 1(a) presents an image of our device taken with an optical microscope. The nanofibers can be seen as faint black lines running between the electrodes. The total length of each nanofiber as estimated from the optical microscope are $\sim 100 \mu\text{m}$ in average. From atomic force microscopy images we estimated the diameter of a single nanofiber as $\sim 120 \text{ nm}$. The average length of MWCNT is $\sim 1.5 \mu\text{m}$. Fig. 1(b) shows a transmission electron microscopy image of the nanofiber. It can be seen that the MWCNTs align inside the nanofiber in series and create a nanochain of conduction with minimal separation. We have three working devices in total. Two working devices out of 25 devices from one sample that were fabricated with 20 wt% MWCNTs and one working device out of 51 devices from two samples that were fabricated with with 25 wt% MWCNTs. The results for the devices discussed, are presented in Fig. 2 and summarized in Table I. Fig. 2 shows the conductance as a function of temperature. As can be seen, the conductance follows a power-law behavior $G(T) \propto T^\alpha$ over a large temperature range as long as the condition $eV \ll k_B T$ is satisfied. For highly resistive devices such as device 2. the drop of the conductance is fast and already in relatively high temperatures the current can no longer be detected. Repeated measurements reveal a Kondo-like behavior in low temperatures and is described elsewhere.²⁵ This may indicate a highly resistive joint

TABLE I. Values for nanofibers used in transport experiments.

	Device 1.	Device 2.	Device 3.
MWCNT % in nanofibers	20	20	25
α	4.6	10.2	2.9
β at min T	4.2	8.6	2.3
G_{305K} (S)	$7.5 \cdot 10^{-7}$	$3 \cdot 10^{-8}$	$2.67 \cdot 10^{-8}$
Diameter (nm)	120	120	120

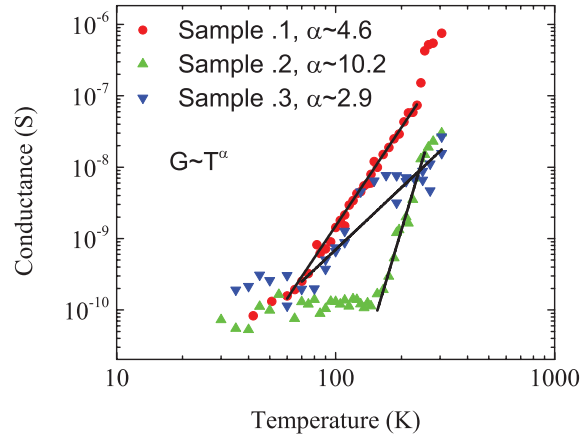


FIG. 2. Conductance vs. temperature for the working devices. The black lines are a fit over the results at high temperatures as expected from the condition $eV \ll k_B T$. All devices obey power-law behavior where in highly resistive devices²⁵ such as in device .2 the conductance drops quickly below the threshold sensitivity of the system. Table I presents the values corresponding to the samples.

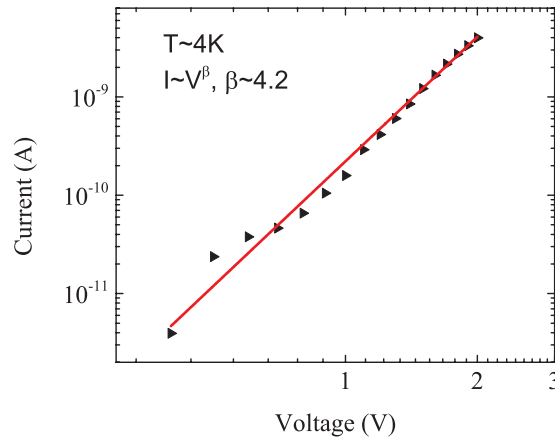


FIG. 3. I-V characteristics at 4K. As can be seen, the power-law behavior of the current under large potential $eV \gg k_B T$ is retained. The red line is a fit of the data with voltages above 0.4 V.

creating a small detachment in the nanochain of conduction. However, device 2. in high temperatures still obeys power-law behavior.

Fig. 3 shows that also the I-V characteristics retain power-law behavior $I(V) \propto V^\beta$ at low temperature where $eV \gg k_B T$ is satisfied. Similar behavior exists in polymer fibers,⁹⁻¹¹ carbon nanotubes,^{1-3,8} quantum Hall edge states,¹⁴ and other inorganic one dimensional nanowires.^{4,12,13}

In carbon nanotube/polymer composite nanofibers beyond a concentration percolation threshold,¹⁸ the electrical conductivity rises sharply to saturation. The dependence between the electrical conductivity to nanotube alignment also obeys similar rules. Beyond the critical

alignment threshold¹⁸ the electrical conductivity shows a sharp rise with respect to the degree of carbon nanotube alignment. For highly aligned carbon nanotubes in composite nanofibers, the onset of percolation pathway begins from loading above 3 wt%.¹⁸ As our loading is 20–25 wt%, we stand well above this threshold. Therefore, the electrospinning process created a nanochain of MWCNTs separated by minimal tunneling barriers (Fig. 1). Hence, we can expect a quasi-one dimensional behavior. However, the length and the morphology of each nanofiber in consideration does not necessarily mean that it would behave similarly to MWCNTs or that the power-law fashion would mean a long nanochain of Luttinger liquid states in series (Fig. 1).

For the confined system we have, there are a few models to consider. The first option is one dimensional variable range hopping^{19,20} and fluctuation induced tunneling.²¹ They predict $\ln G \sim -1/T^p$, which contradict the temperature dependence observed experimentally. The discrepancy between our results to the fluctuation induced tunneling^{21,22} model exemplifies the fact that the separation between the consecutive MWCNTs is minimal (Fig. 1). For three-dimensional disordered system²³ in the critical regime of the metal-insulator transition, the temperature dependence of the resistivity follows a universal power-law $\sigma(T) \sim T^\gamma$ with $0.33 < \gamma < 1$. In our case all power-law exponents exceed unity (Table I) and therefore this model is invalid. We also rule out space-charge limited current²⁴ where $I \sim V^\beta$ with $\beta \sim 2$. According to our fits $\beta \gg 2$ (Table I and Fig. 3), which is in contradiction to this explanation.

Turning to the model of Wigner crystal- it is caused by long range Coulomb interaction and occurs in solids with a dilute system of electrons such as carbon nanotubes⁶ where the Coulomb energy E_C is bigger than the kinetic energy of the electrons E_F . As our structure is comprised of consecutive MWCNTs divided by tunneling barriers and impurities (Fig. 1) -this morphology can easily create potential wells where electrons get trapped and create Wigner crystal. Every Wigner crystal state would be pinned down by the tunneling insulating barriers, impurities and kinks. However, since each potential well is essentially a MWCNT with small energy gap (< 100 meV), it would be difficult to observe any Wigner crystal state. At this time, we cannot fully explore this behavior at low temperature. A classical Wigner crystal, on the other hand, would require an exponential relation for the conductance with temperature¹⁹ in low temperatures and one dimensional variable range hopping behavior. This is not recorded in our system.

To be consistent with Luttinger liquid behavior the system must follow a few requirements: power-law of the current under large potential $eV \gg k_B T$ and of the conductance at small potential $eV \ll k_B T$. The number of the channels in the nanofiber decide on the power-law parameters of β and α . More generally, the Luttinger liquid model states the current depends^{1-3,6,8} on voltage and temperature as

$$I = I_0 T^{\alpha+1} \sinh(eV/k_B T) |\Gamma(1 + \beta/2 + ieV/\pi k_B T)|^2, \quad (1)$$

where Γ is the Gamma function, I_0 is a constant, and α and β are the power-law parameters introduced above. Fig. 4 shows how at low temperatures the current follows a universal curve. This agrees with the Luttinger liquid model described by Eq. (1). The Luttinger liquid model characterizes a system by its interaction parameter g derived from the tunneling density of states.^{1,3} For strong repulsive electron-electron interactions, $g \ll 1$ while for non interacting electrons, $g = 1$. According to Luttinger liquid theory predictions for a system where impurity and kink barriers are dominant α follows:

$$\alpha \sim (g^{-1} - 1)/4. \quad (2)$$

We estimate $g_1 \sim 0.04$, $g_2 \sim 0.02$, $g_3 \sim 0.08$ respectively for the devices under consideration (A similar value can be reached also for intertube tunneling). This indicates a strong repulsive electron-electron interactions regime in the nanofibers.

For a single conduction channel, e.g. at low temperatures where only few channels survive and are active, the correlation between the power-law exponents is

$$\beta = 1 + \alpha. \quad (3)$$

In our measurements β is always lower than $\alpha + 1$ as already observed in inorganic nanowires and polymer nanowires.^{9,12} The absolute values of α and β determined by us are also higher

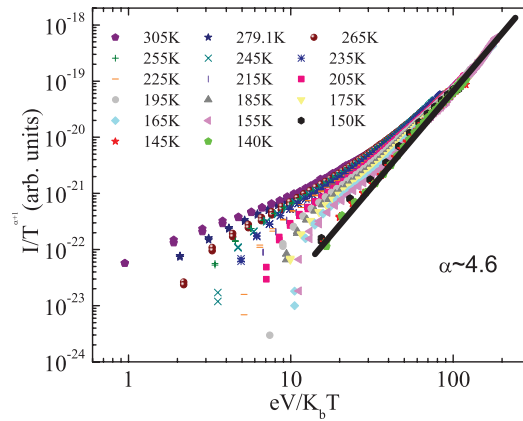


FIG. 4. $I/T^{\alpha+1}$ vs. $eV/k_B T$ plot for different temperature where α value is taken from a fit of $G(T) \propto T^\alpha$ (Table I). At low temperatures the curves gather up into a universal line as Eq. (1) predicts. The continuous black line accentuates the universal line. The figure of device 1. is presented.

than of MWCNTs^{3,7} ($\alpha, \beta \sim 0.3$); again, they are close to those found in conjugated conducting polymer nanowires⁹ and long InSb nanowires.¹² Observing characteristics resembling Luttinger liquid behavior is quite striking, since our devices are ultra-long and composed of many segments divided by insulating barriers. This apparent strong confinement is probably due to the morphology of the nanofiber. Comparing our result to nanotube devices with a single kink¹ where $\alpha \sim 2.2$ or polymer nanowire device⁹ where $\alpha \sim 2.8$, we can see that the value of $\alpha \sim 2.9$ for device 3. is close to these results despite its size. Our devices are clearly rich with kinks and impurities along their long course. Every kink, impurity and PMMA barrier mark another tunneling barrier between consecutive Luttinger liquid states (Fig. 1). It is no wonder then, that for devices 1. and 2. we get higher values of α and strong power-law dependence.

Finally, we discuss environmental Coulomb blockade. Basically, in the limit of a multichannel device, environmental Coulomb blockade corresponds with Luttinger liquid which for many modes in parallel predicts a power-law behavior⁷ as well. We consider the disordered conductor as an effective LC transmission line, which was found to be valid for MWCNT in the range of not too small voltages,⁷ $eV \gg k_B T$. Considering our nanofiber as a lumped transmission line and neglecting the resistive part yields an impedance $Z = n\sqrt{L/C}$, where n is the number of joints in series (Fig. 1) inside the nanochain of conduction, $L \sim 1 \text{ nH}/\mu\text{m}$ is the kinetic inductance of a single MWCNT and $C \sim 30 \text{ aF}/\mu\text{m}$ typical value of the capacitance of a single MWCNT.⁷ For the most conductive device 3. with the lowest α , $Z \sim 275 \text{ K}\Omega$ at 10 K (where $eV \gg k_B T$). From this we find $n \sim 50$. This is consistent with the length of our device $\sim 100 \mu\text{m}$ and the average length of the MWCNT ($1.5 \mu\text{m}$).

For single MWCNT the exponent for tunneling into the bulk of a nanotube α_{bulk} . Bulk tunneling can be used as a building block to derive other exponents.⁷ For example tunneling to the end of Luttinger liquid state $\alpha_{end} = 2\alpha_{bulk}$. A theoretical value for α_{bulk} was calculated⁷ 0.02–0.08. Since in our nanofibers the conduction channels are connected in series (Fig. 1), we consider n as the number of joints in the nanochain and correspondingly $\alpha \sim n \cdot \alpha_{bulk}$. For the lowest value of $\alpha \sim 2.9$ we get $\alpha_{bulk} \sim 0.06$. This agrees with the theoretical predictions.⁷ We note, however, that previous experimental results⁷ found higher values for α_{bulk} .

In conclusion, we showed quasi-one dimensional transport behavior in electrospun nanofibers. We found that the conductance behaves as power-law from room temperature down to $\sim 60 \text{ K}$. The I-V curve is also described by a power-law. These characteristics are a fingerprint for one dimensional transport systems with Luttinger liquid or environmental Coulomb blockade. Therefore, we have constructed a device made of many Luttinger liquid states in series which behaves as an effective lumped LC transmission line. Despite the obvious similarities to a single MWCNTs and polymer nanowires, it bears many differences that still need to be resolved.

ACKNOWLEDGMENTS

The authors would like to acknowledge T. Schurig and C. Assman from Physikalisch-Technische Bundesanstalt for allowing access to their facilities. The authors thank S. Reich from Freie Universität Berlin for fruitful discussions. Parts of this work were supported by the European Research Council under grant number 210642.

- ¹Z. Yao, H. W. C. Postma, L. Balents, and C. Dekker, "Carbon nanotube intramolecular junctions," *Nature* **402**, 273–276 (1999).
- ²B. Gao, A. Komnik, R. Egger, D. C. Glattli, and A. Bachtold, "Evidence for luttinger-liquid behavior in crossed metallic single-wall nanotubes," *Phys. Rev. Lett.* **92**, 216804 (2004).
- ³M. Bockrath, D. H. Cobden, J. Lu, A. G. Rinzler, R. E. Smalley, L. Balents, and P. L. McEuen, "Luttinger-liquid behaviour in carbon nanotubes," *Nature* **397**, 598–601 (1999).
- ⁴S. Zaitsev-Zotov, Y. Kumzerov, Y. Firsov, and P. Monceau, "Unconventional magnetoresistance in long insb nanowires," *Journal of Experimental and Theoretical Physics Letters* **77**, 135–139 (2003).
- ⁵A. Choi, K. H. Kim, S. J. Hong, M. Goh, K. Akagi, R. B. Kaner, N. N. Kirova, S. A. Brazovskii, A. T. Johnson, D. A. Bonnell, E. J. Mele, and Y. W. Park, "Probing spin-charge relation by magnetoconductance in one-dimensional polymer nanofibers," *Phys. Rev. B* **86**, 155423 (2012).
- ⁶V. V. Deshpande and M. Bockrath, "The one-dimensional wigner crystal in carbon nanotubes," *Nat Phys* **4**, 314–318 (2008).
- ⁷A. Bachtold, M. de Jonge, K. Grove-Rasmussen, P. L. McEuen, M. Buitelaar, and C. Schönenberger, "Suppression of tunneling into multiwall carbon nanotubes," *Phys. Rev. Lett.* **87**, 166801 (2001).
- ⁸E. Graugnard, P. J. de Pablo, B. Walsh, A. W. Ghosh, S. Datta, and R. Reifengerber, "Temperature dependence of the conductance of multiwalled carbon nanotubes," *Phys. Rev. B* **64**, 125407 (2001).
- ⁹A. N. Aleshin, "Quasi-one-dimensional transport in conducting polymer nanowires," *Physics of the Solid State* **49**, 2015–2033 (2007).
- ¹⁰A. N. Aleshin, H. J. Lee, S. H. Jhang, H. S. Kim, K. Akagi, and Y. W. Park, "Coulomb-blockade transport in quasi-one-dimensional polymer nanofibers," *Phys. Rev. B* **72**, 153202 (2005).
- ¹¹A. N. Aleshin, H. J. Lee, Y. W. Park, and K. Akagi, "One-dimensional transport in polymer nanofibers," *Phys. Rev. Lett.* **93**, 196601 (2004).
- ¹²S. V. Zaitsev-Zotov, Y. A. Kumzerov, Y. A. Firsov, and P. Monceau, "Luttinger-liquid-like transport in long insb nanowires," *Journal of Physics: Condensed Matter* **12**, L303 (2000).
- ¹³E. Levy, I. Sternfeld, M. Eshkol, M. Karpovskii, B. Dwir, A. Rudra, E. Kapon, Y. Oreg, and A. Palevski, "Experimental evidence for luttinger liquid behavior in sufficiently long gaas v-groove quantum wires," *Phys. Rev. B* **85**, 045315 (2012).
- ¹⁴A. M. Chang, L. N. Pfeiffer, and K. W. West, "Observation of chiral luttinger behavior in electron tunneling into fractional quantum hall edges," *Phys. Rev. Lett.* **77**, 2538–2541 (1996).
- ¹⁵V. Datsyuk, M. Lisunova, M. Kasimir, S. Trotsenko, K. Gharagozloo-Hubmann, I. Firkowska, and S. Reich, "Thermal transport of oil and polymer composites filled with carbon nanotubes," *Applied Physics A* **105**, 781–788 (2011).
- ¹⁶J.-S. Kim and D. H. Reneker, "Polybenzimidazole nanofiber produced by electrospinning," *Polymer Engineering & Science* **39**, 849–854 (1999).
- ¹⁷B. M. wall Carbon Nanotubes, N. Processing, and D. Product, "Baytubes C 150 P," (2010).
- ¹⁸F. Du, J. E. Fischer, and K. I. Winey, "Effect of nanotube alignment on percolation conductivity in carbon nanotube/polymer composites," *Phys. Rev. B* **72**, 121404 (2005).
- ¹⁹M. M. Fogler, S. Teber, and B. I. Shklovskii, "Variable-range hopping in quasi-one-dimensional electron crystals," *Phys. Rev. B* **69**, 035413 (2004).
- ²⁰T. Hu and B. I. Shklovskii, "Hopping conductivity of a suspension of flexible wires in an insulator," *Phys. Rev. B* **74**, 174201 (2006).
- ²¹H. Xie and P. Sheng, "Fluctuation-induced tunneling conduction through nanoconstrictions," *Phys. Rev. B* **79**, 165419 (2009).
- ²²B. Sundaray, A. Choi, and Y. W. Park, "Highly conducting electrospun polyaniline-polyethylene oxide nanofibrous membranes filled with single-walled carbon nanotubes," *Synthetic Metals* **160**, 984–988 (2010).
- ²³D. Khmel'nitskii and A. Larkin, "Mobility edge shift in external magnetic field," *Solid State Communications* **39**, 1069–1070 (1981).
- ²⁴J. N. Coleman, S. Curran, A. B. Dalton, A. P. Davey, B. McCarthy, W. Blau, and R. C. Barklie, "Percolation-dominated conductivity in a conjugated-polymer-carbon-nanotube composite," *Phys. Rev. B* **58**, R7492–R7495 (1998).
- ²⁵A. Avnon, V. Datsyuk, S. Trotsenko, B. Wang, S. Zhuo, N. Grabbert, and H.-D. Ngo, "Zero Bias anomaly in an individual suspended electrospun nanofiber," (2013), manuscript under submission.